The dynamics of vortex structures and states of current in plasma-like fluids and the electrical explosion of conductors: II. Computer experiment

1993 J. Phys. A: Math. Gen. 26 6649

(http://iopscience.iop.org/0305-4470/26/23/015)

J. Phys. A: Math. Gen. 26 (1993) 6649–6665. Printed in the UK

The dynamics of vortex structures and states of current in plasma-like fluids and the electrical explosion of conductors: II. Computer experiment

N B Volkov and A M Iskoldsky

Russian Academy of Science, Ural Division, Institute of Electrophysics, 34 Komsomolskaya St., Yekaterinburg 620219, Russia

Received 4 September 1992, in final form 20 September 1993

Abstract. In the present paper which is the second in a series, the dynamics of non-equilibrium phase transitions and states of current in electrophysical systems providing an external circuit and a nonlinear element, the model of which has been developed in the first paper of the series (in the development of the model local kinetic transport coefficients were assumed to be constant), has been analysed and simulated. A non-equilibrium phase transition has been shown to be induced by large-scale hydrodynamic fluctuations (vortex structures). Critical exponents of the amplitude's singular behaviour (the order parameters) for three types of circuit have been determined. Non-equilibrium phase transitions induced by external harmonic noise with a random or deterministic phase have been studied. The detuning between the external noise frequency and natural frequencies of a nonlinear element determined by large-scale hydrodynamic fluctuations have been shown to give rise to random oscillations, which are typical of a strange attractor. When the frequencies coincide, a limit cycle appears in the system, which is characterized by the fact that the phase trajectory does not fill the phase space completely.

1. Introduction

In the first paper of this series [1], a dynamic model of a non-equilibrium phase transition (NPT) has been offered and studied. This model, in our opinion, describes the initial stage of the turbulence nucleation in a conducting fluid (see our paper [2] which indicates an analogy between the initial stage of the electrical explosion of a conductor (EEC) and the turbulence nucleation in an incompressible liquid). It was also noted in [1] that a further evolution of vortex structures, corresponding to a transition to an isotropic spectrum, which is characteristic of a developed turbulence, would be a consequence of the splitting of the space scale. Assuming that the splitting is absent or hindered (as follows from [1], for the splitting to take place, the existence of a laminar flow of fluid is essential), then already in the framework of model [1], general problems of the dynamics of states of current in a conducting liquid can be studied, particularly, the dynamics of a transition to a steady state of the turbulence resistance. The model of [1] is a model of a nonlinear element (NE) inserted into the electric circuit that is a thermostat with respect to the NE.

The purpose of the present computer experiment was to study proper motions that appear in the dynamic system, consisting of the NE model and the electric circuit, the dynamics of a spontaneous symmetry breaking in the initially laminar electron fluid, and also the NPT dynamics, induced by either a deterministic or a stochastic external noise.

0305-4470/93/236649+17$07.50

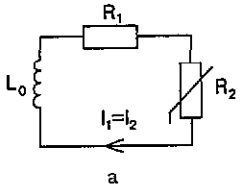

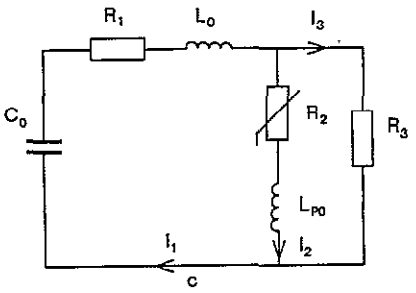

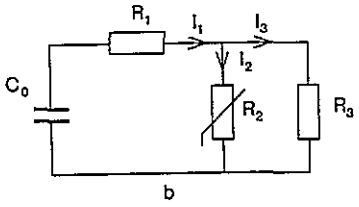

Figure 1. Electric circuits: (*a*) circuit S1, (*b*) S2 and (*c*) S3. The following notation is used: L_0 inductance; C_0 capacitance; R_1 ballast resistance; R_2 the resistance of a nonlinear element; L_{p0} its external inductance; R_3 load impedance. Circuit S1 can easily be transformed to the DC current source if we formally let $L_0 \to \infty$. Similarly, circuits S2 and S3 can easily be transformed to the DC voltage sources if we formally let $C_0 \to \infty$.

2. Equations and procedure

We discuss three types of external electric circuit: S1 (figure 1(*a*)), S2 (figure 1(*b*)) and S3 (figure 1(*c*)), where I_1, I_2 and I_3, are the currents in the corresponding branches of a network (see the figure caption for details of other notation). Circuit S1 can easily be transformed to the DC current source if we formally let $L_0 \to \infty$. Similarly, circuits S2 and S3 can easily be transformed to the DC voltage sources if we formally let $C_0 \to \infty$.

Equations describing transition processes in the circuits are:

A. The model of a nonlinear element.

$$\dot{X} = s(-X + I_2 Y) \tag{1}$$

$$\dot{Y} = a_1 X(-Z + a_1 r_1 I_2) - Y \tag{2}$$

$$\dot{Z} = -(a_1 XY + bZ) \tag{3}$$

where the point symbol '˙' stands for the differentiation operator of a dimensionless time $\tau = t t_0^{-1}$, $t_0 = (4 g_1^2 \nu_m)^{-1} b r_0^2$ is the basis time; $I_2 = i_2 I_0^{-1}$ is the dimensionless current; $r_1 = R R_c^{-1}$ is the control parameter of the model; $a_1 = \pi g_1^{-1} = 0.819$; $g_1 = 3.83171$ corresponds to the first zero of the Bessel function $J_1(x)$; $b = \frac{8}{3}$; R and R_c are, respectively, the magnetic Rayleigh number and its critical value.

As was noted in [1], knowing $X(\tau)$, $Y(\tau)$, $Z(\tau)$, and $I(\tau)$ enables determination of the paths of particles transferring mass ('hydrodynamic particles') and current (conduction electrons), while solving the motion equations

$$\dot{R}_a = -C_r X \cos(\pi k Z_a) J_1(g_1 R_a) \tag{4}$$

$$\dot{Z}_a = C_z X \sin(\pi k Z_a) J_0(g_1 R_a) \tag{5}$$

and

$$\dot{R}_e = \sqrt{2} B k r_1^{-1} Y \sin(\pi k Z_e) J_1(g_1 R_e) \tag{6}$$

$$\dot{Z}_e = B\left[2I_2 + (a_1 r_1)^{-1}\left(\sqrt{2} Y \cos(\pi k Z_e) J_1(g_1 R_e) + 2Z(J_1^2(g_1 R_e) - J_0^2(g_1 R_e))\right)\right] \tag{7}$$

where R_a, Z_a and R_e, Z_e are the coordinates of the paths for atoms and conduction electrons respectively; $C_r = 2^{1/2}\pi g_1^{-2}$; $C_z = g_1 k^{-1} C_r$; $B = bcH_0(16\pi e n_e \nu_m g_1^2)^{-1}$; e and n_e are the unit charge and the conduction electron density, respectively. Since (4)–(7) determine the particle paths corresponding to each moment of time τ, then in their integration the X, Y, Z and I amplitudes should be regarded as constant, i.e. sets (4)–(5) and (6)–(7) are autonomous dynamic systems of second order on the plane (r, z).

B. Circuit S1.

$$\dot{I}_2 = -[\Pi_1 I_2 + \Pi_2(I_2 - a r_1^{-1} Z)] \tag{8}$$

where $\Pi_1 = R_1 c^2 t_0 L_0^{-1}$, $\Pi_2 = R_{p0} c^2 t_0 L_0^{-1}$ and $a = \pi^{-1} J_0^2(g_1)$.

C. Circuit S2.

$$\dot{U} = -\Pi_4 I_1 \tag{9}$$

$$\dot{I}_2 = G_2^{-1}[U + G_1 \Pi_2 a r_1^{-1} Z] \tag{10}$$

$$\dot{I}_1 = (1 + \Pi_2 \Pi_3^{-1}) I_2 \tag{11}$$

where $\Pi_2 = R_{p0} R_1^{-1}$, $\Pi_3 = R_3 R_1^{-1}$, $\Pi_4 = t_0(R_0 C_0)^{-1}$, $G_1 = 1 + \Pi_3^{-1}$ and $G_2 = 1 + G_1 \Pi_2$.

D. Circuit S3.

$$\dot{I}_1 = \Pi_5 U - [\Pi_1 I_1 + \Pi_6 \dot{I}_2 + U_R] \tag{12}$$

$$\dot{U} = -\Pi_4 I_1 \tag{13}$$

$$\dot{I}_2 = \Pi_6^{-1}[\Pi_3(I_1 - I_2) - U_R] \tag{14}$$

where $U_R = \Pi_2(I_2 - a r_1^{-1} Z)$, $\Pi_1 = R_1 c^2 t_0 L_0^{-1}$, $\Pi_2 = R_{p0} c^2 t_0 L_0^{-1}$, $\Pi_3 = R_3 c^2 t_0 L_0^{-1}$, $\Pi_4 = I_0 t_0 (U_0 C_0)^{-1}$, $\Pi_5 = U_0 c^2 t_0 (I_0 L_0)^{-1}$, $\Pi_6 = L_{p0} L_0^{-1}$ and U_0, I_0 are the basis voltage and the current. If we choose U_0 and I_0 so that $U_0 = R_1 I_0$, then $\Pi_1 = \Pi_5$ and $\Pi_4 = t_0(R_1 C_0)^{-1}$. From (9)–(14) one can see that the circuit with a DC voltage corresponds to $\Pi_4 = 0$. The initial condition for (8) is $I_2(0) = 1$ and for (9) it is $U(0) = 1$. Correspondingly, for (12)–(14), the initial conditions are of the form $I_1(0) = I_2(0) = 0$, $U(0) = 1$. To diminish the arbitrariness in choosing initial conditions for (1)–(3), we take one of the values on the surface of stable solutions of (1)–(3) at $I_2 = 1 =$ constant: $X(0) = Y(0) = -1.1419$, $Z(0) = -0.40048$. In computer experiments, we set $s = \nu_m \nu^{-1} = 0.3779 \times 10^{-3}$ in practically all the cases (below, other values of $X(0)$, $Y(0)$, $Z(0)$ and s are marked clearly).

It can be shown that (1)–(3) and (8), and also (1)–(3) and (9)–(11), (1)–(3) and (12)–(14), without a load resistor, exhibit an asymptotic behaviour similar to that of equation (50) in [1]. Actually, for circuit S1 and also for a one-loop circuit S3, we obtain (below, t_* is the time corresponding to the singularity)

$$X \sim -1.8315(t_* - t)^{-1} \tag{15}$$

$$Y \sim Z \sim -0.9569\mathrm{i}(r_1(as\Pi_2)^{-1})^{1/2}(t_* - t)^{-1} \tag{16}$$

$$I_2 \sim -1.9139\mathrm{i}(a\Pi_2(r_1 s)^{-1})^{1/2}(t_* - t)^{-1/2}. \tag{17}$$

Similar asymptotes for a one-loop circuit have the following form

$$X \sim -1.221(a\Pi_2 G_3 G_4^{-1})^{1/2}(t_* - t)^{-1} \tag{18}$$

$$Y \sim 1.105\mathrm{i}(G_3(as\Pi_2)^{-1})^{1/2}(t_* - t)^{-1} \tag{19}$$

$$Z \sim 1.105\mathrm{i}G_3 G_4^{-1/2}(t_* - t)^{-1} \tag{20}$$

$$I_2 \sim 1.105\mathrm{i}a\Pi_2 r_1^{-1}(sG_4)^{-1/2}(t_* - t)^{-1} \tag{21}$$

$$U \sim 1.105\mathrm{i}a\Pi_2\Pi_4 r_1^{-1}(sG_4)^{-1/2}\ln(t_* - t) \tag{22}$$

where $G_3 = 1 + \Pi_2$, $G_4 = G_3(a\Pi_2)^{-1} - a_1$. The imaginary unit i in (15)–(22) points to a fluctuating character of transition processes in circuits S1–S3. It is worthwhile noticing that without NE in circuits S1 and S2, a fluctuating process is impossible.

We noted above that, knowing the X, Y, Z and I amplitudes, we can plot spatial field distributions of hydrodynamical ($u(r, z)$) and current ($u_T(r, z)$) velocities at any point of time. Therefore it is necessary to solve (4)–(5) and (6)–(7).

Equations (1)–(3), (4)–(5), (6)–(7) and (8)–(14) are dynamic systems which are in general non-autonomous. Therefore, to study them, a mathematical technique of the theory of dynamic systems [3–7] can by employed. In particular, one of the methods used below is that of Lyapunov's characteristic exponents [8, 9]. Despite the fact that equations (1)–(14) describe physical processes in an open dissipative system, this, as will be shown below, refers to the class of mixing dynamic systems (K-systems [10, 11]), determining relaxation to a thermodynamic equilibrium [11]. If instant values of Lyapunov's exponents are regarded as time-averaged logarithms of Yakobian's eigenvalue modules of a linearized dynamic system, then these exponents can be used to analyse a transition chaos in the dynamic system and the time behaviour of the phase-space fractal dimensionality and also of the Kolmogorov–Sinai metrical entropy, related to the positive Lyapunov exponents $\{\lambda_i{}^+\}$ by $S = \sum_i \lambda_i{}^+$ [4], can be found. To calculate Lyapunov's exponents we use the algorithm proposed in [8, 9] and to calculate fractal dimensionality we use the Kaplan–Yorke formula [12] $d_L = j + \sum_{i=1}^{j} \lambda_i |\lambda_{i+1}|^{-1}$, where j is evaluated from the conditions $\sum_{i=1}^{j} \lambda_i > 0$ and $\sum_{i=1}^{j+1} \lambda_i < 0$. Below, parallel with the Kolmogorov–Sinai entropy S, we use the value $F = \sum_i \lambda_i$. Computer experiments show that in our dynamic system the case of all the Lapunov exponents being positive is realized. Here, by comparing S and F, we can find a characteristic time when the behaviour of the process changes, i.e. the so-called explosive regime appears.

A characteristic property of the dynamic systems described by (1)–(3) and (8)–(14) is the existence of a one-to-one phase-space mapping onto the plane U–I, which is sometimes called a UI-characteristic (VCC—it should be noted that, strictly speaking, the notion of VCC is applicable only for a stationary state of the dynamic system). With a uniform step of the amplitude mapping in time (Δt), VCC can be regarded as the Poincaré point mapping (accurate within the step Δt). There is a stationary state at a DC voltage in the circuit S2; also an analytical expression for VCC can be found for this circuit. Actually, the current in NE is determined by the following expression

$$I_2 = C_1 + C_2 r_1^{-1} Z \tag{23}$$

($C_1 = UG_2^{-1}$, $C_2 = G_1\Pi_2 a_3 G_2^{-1}$), therefore VCC takes the form

$$U_2 = \Pi_2(1 - a_3 C_2^{-1})I_2 + \Pi_2 a_3 C_1 C_2^{-1}. \tag{24}$$

A stationary solution for circuit S2 at $\Pi_4 = 0$ has the form

$$X_\infty = \pm(-bZ_\infty I_{2\infty} a_1^{-1})^{1/2} \tag{25}$$

$$Y_\infty = \pm(-bZ_\infty (a_1 I_{2\infty})^{-1})^{1/2} \tag{26}$$

$$Z_\infty = -\frac{r_1 C_1(1-2a_1C_1)}{2C_2(1-a_1C_2)}\left\{1+\left(1-\frac{4C_2(1-a_1^2C_1^2r_1)(1-a_1C_2)}{a_1C_1^2r_1(1-2a_1C_1)^2}\right)^{1/2}\right\} \tag{27}$$

where $I_{2\infty}$ is determined by formula (23). It is seen from (27) that at negative root values a stationary solution is non-existent. Expressions (25) and (26) point to the existence of two stationary solutions in the circuit S2 which differ in X_∞ and/or Y_∞ signs.

3. Computer experiment and discussion

In our computer experiment we investigated the following problems:

(1) To find out how initial data influence the dynamics of processes in the dynamic systems under study and also the role they play in reaching and choosing a stationary state from a set of permissible stationary states.
(2) To study the spectral dynamics of Lyapunov's exponents and the Kolmogorov–Sinai entropy and also the role of transition chaos in 'forgetting' the initial condition.
(3) To investigate the dynamics of establishing a limiting cycle in circuit S3 under a DC voltage and its connection with the initial data.
(4) To find out the difference between physical processes occurring in the dynamic systems with a finite energy content (circuits S1 and S3) and those in circuits under a DC voltage (circuits S2 and S3).
(5) To analyse the problem of transformation of the time in the model (1) and to study the chaos in a 'transformed' dynamic system.
(6) To determine and to classify the characteristic features of a spontaneous symmetry breaking and the transition to turbulent resistance in the initially laminar electron fluid.
(7) To study the dynamics of NPT induced by an external noise (deterministic or chaotic) and also the influence of frequency detuning on the transition process in the circuit S3.

Presented below are the principal results of our computer experiment and their brief discussion.

The dynamics of transition processes has been found to be of a threshold character, a transition to a steady-state regime occurring through a sequence of bifurcations at a sufficient level of supercriticality. In this case, the transition process in circuits S1 and S2 is an oscillating one and a section with a negative differential resistance appears on the VCC. Figure 2 displays VCC in the circuit S1. One can see that, for a critical regime, the system 'wishes' to perform a phase transition, though due to the lack of supercriticality the initiated perturbations subside and the system comes back into the steady state, corresponding to zero current in circuit S1.

In the circuit S2 under a DC voltage there is a stationary state determined by expressions (25)–(27). A transition to this state occurs through a sequence of bifurcations (curves 1 and 2 in figure 3 show, respectively, the change in the current and the voltage drop across NE). Let us note that without NE in the circuit S1 the fluctuating process fails. The fluctuations appear due to the fact that NE is actually a dissipative electrodynamic system where energy transforms step-by-step from mechanical degrees of freedom to the electromagnetic field

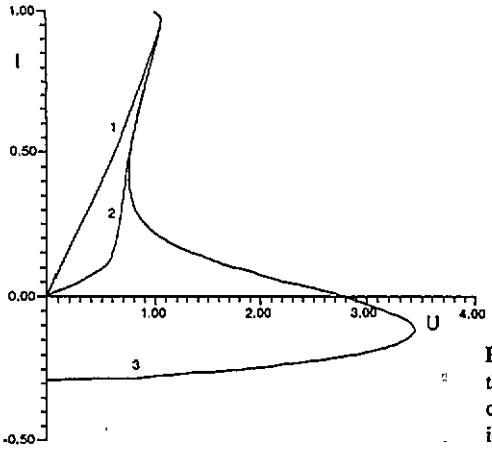

Figure 2. UI-characteristics of a nonlinear element in the circuit S1: curve 1, subcritical conditions ($r_1 = 5$); curve 2, critical conditions ($r_1 = 6.34$); curve 3, supercriticality ($r_1 = 6.5$).

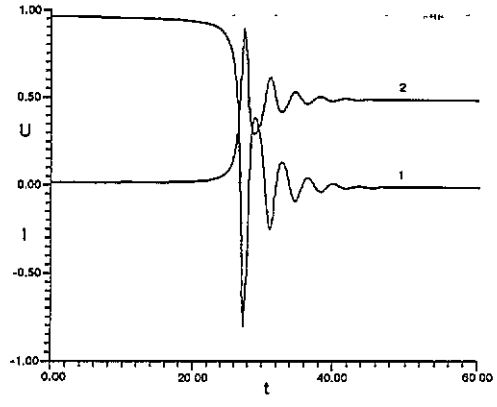

Figure 3. Characteristics of the transition process in the circuit S2 with a DC voltage source: curve 1, current in the nonlinear cell; curve 2, voltage in the nonlinear cell. In circuit S2, at a constant R_2, oscillations are impossible. The oscillations shown in the figure are the result of their own internal motion in the nonlinear element.

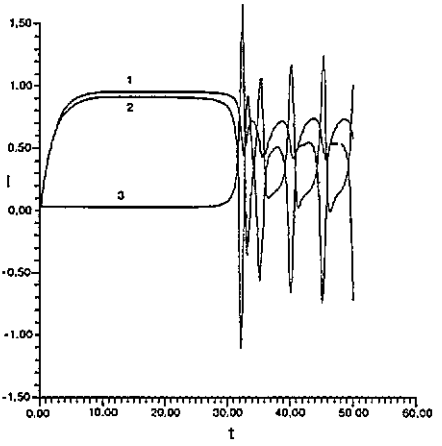

Figure 4. Characteristics of the transition process in the circuit S3 with a DC voltage source: curve 1, the total current; curve 2, current in the nonlinear cell; curve 3, a load current. Adding the L_0 and L_{p0} inductances to circuit S2 results in the destruction of the stationary state obtained in circuit S2. Instead, the limit cycle acts in circuit S3.

and *vice versa* (see [1]). The stationary state corresponds to a practically zero current in NE, the amplitude of which is sufficient to sustain this regime, the voltage drop across the conductor being non-zero. The NE resistance in the stationary state surpasses considerably its initial value. Next we show that it is determined by the formation of vortex structures in the electron fluid (by a spontaneous symmetry breaking), which is why it can be referred to as a turbulent resistance.

As follows from expressions (25)–(27), the VCC corresponds to two stationary states which differ in the X and (or) Y signs. The realization of one of the signs is determined by $X(0)$ and (or) $Y(0)$. Our simulation showed that the initial state of the system with the signature $\{---\}$ or $\{--+\}$, $\{--0\}$ or $\{-+0\}$ leads to the choice of the stationary state with the signature $\{---\}$. The initial state with $\{++-\}$ or $\{+--\}$, $\{++0\}$ or

$\{+-0\}$ results in the choice of the stationary state, respectively, with $\{++-\}$ (the symbol 0 denotes that $Z(0) = 0$ and, hence, its sign is neutral). It has also been shown that the signature of the stationary state, when $X(0) = Z(0) = 0$, is determined by the sign of $Y(0)$: the signature $\{---\}$ corresponds to the signature of the initial state $\{0-0\}$, and the signature $\{0+0\}$ corresponds to $\{++-\}$.

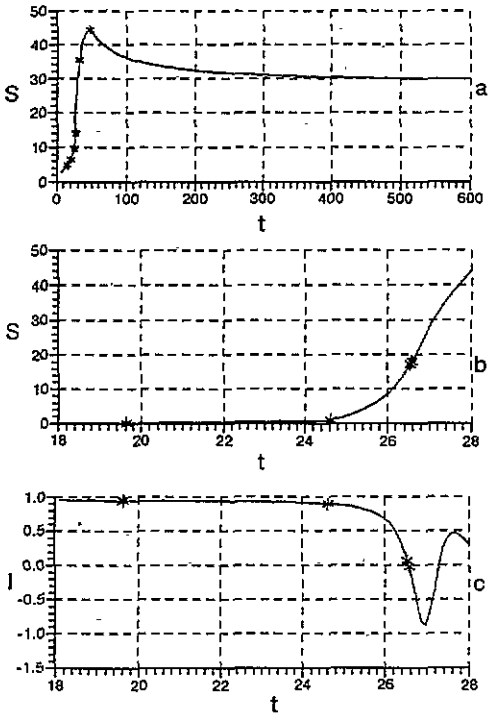

Figure 5. Time variation of the Kolmogorov–Sinai entropy $S(t)$ and the current in the nonlinear cell for circuit S2 with a DC voltage source: (*a*) $S(t)$; (*b*) the starting section of the curve $S(t)$; (*c*) the starting section of the current curve; the sign * marks characteristic points for which sections of the conductor are drawn in the plane r–z (figure 9): the second point corresponds to the break of the curve $S(t)$ when all the Lyapunov exponents are non-negative ($I_2 = 0.9$: the beginning of switching); and the third point to the inflection point $S(t)$ ($I_2 \cong 0.1 - 0.15$: the end of switching). The maximum $S(t)$ corresponds to the maximum transition chaos (to the minimum time for tripping the correlation $\tau_c \sim S^{-1}$ [13]).

A similar condition takes place in the circuit S3 under a DC voltage. The presence of reactance elements in the circuit, i.e. the inductance L_0 and L_{p0}, brings about the distortion of the stationary state that existed in circuit S2. A limit cycle acts as a stationary state in circuit S3 (see figure 4).

The stationary solution in circuit S2 and the limit cycle in circuit S3 at fixed circuit parameters 'forget' about the starting data due to bifurcations in the dynamic system (the starting data influence the time of transition to the stationary state rather than the stationary state itself). The character of forgetting the starting data is characterized by the time of uncoupling the correlations τ_c, which is connected with the Kolmogorov–Sinai entropy by the relation $\tau_c \sim S^{-1}$ [10, 13]; the entropy, in turn, is determined by the spectrum of the Lyapunov exponents. Figure 5 shows the entropy time alteration for circuit S2; the star symbol $*$ marks characteristic moments of time corresponding to the cross sections of the conductor passed by the plane r–z in figure 9. The maximal entropy growth rate, and, hence, the maximal rate of the descent of τ_c, fall at the region of a transition chaos, which corresponds to the process when the system passes through successive bifurcations. Figure 5 shows the initial section $S(t)$ where, among the points marked by $*$, there are two characteristic points: the first one corresponds to the time when all the Lyapunov exponents become non-zero (positive) and the derivative $S(t)$ is discontinuous; the second one corresponds to the inflection point of the curve $S(t)$. The breakpoint corresponds to

the current 0.9 and the inflection point to 0.1–0.15 (see figure 5(*c*) which shows the curve of current in NE). This allows us, as is shown in the third paper of the present series, to formalize the notion of the 'start' and the 'end' of commutation, while processing the experimental findings. The maximum on the entropy curve (figure 5(*a*)) corresponds to a maximal chaos. On reaching this chaos the system 'settles down' and $S(t)$ tends to a certain limit, which, generally speaking, depends on the point in phase space from which we start at the initial moment. Under fixed circuit parameters, as is shown by computer experiment, the stationary state corresponds to an infinite set of starting data (trajectories). This behaviour is characteristic of dynamic systems with mixing (K-systems) [4, 10, 11, 13].

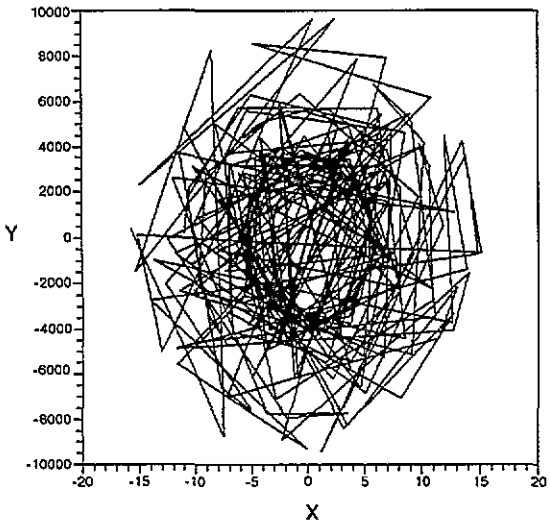

Figure 6. Mapping of the phase trajectory of *the amplitude $X(t)$ and $Y(t)$ plane obtained in* circuit S2 with a DC voltage source and the nonlinear element in the model in which the time sign is replaced by the opposite sign (a nonlinear element with backward running time).

In the indicated set of trajectories, there is one (in the sense of an optimal control [14]) in the ε vicinity, where the Kolmogorov–Sinai entropy is minimal. Therefore it can be called geodesic. We found it by converting the time in the initial equations of the model (it should be noted that we were prompted to do so by the comments in [13] that the state with all Lyapunov exponents positive corresponds to a repelling centre—a repeller [4]; in this case the state at $t = -\infty$ corresponds to an attractor). We expected that, having passed through the region of transition chaos, the system returns to the state close to the initial one. However this assumption proved to be wrong. In the dynamic system obtained by converting the time, when it approaches the onset of the region of a transition chaos, chaos appears in the cross section of the phase transition in the X–Y plane (figure 6). Since NE are included in the circuit with a DC voltage source, the X, Y, Z and I amplitudes tend to infinity during a finite time 'covering up' the whole region of the phase transition. Starting from any point on this trajectory we come back to the stationary state directly along this line (see figure 7, which shows the change in X (*a*), Y (*c*) at the backward running time, and X (*b*), Y (*d*) at the forward time). Starting from any other trajectory point except the geodesic one, we will also come to the stationary state, though along another trajectory, which eventually will tend to a geodesic one; in this sense a geodesic trajectory is an attractor (see figure 8).

Polarity reversals of the current occurring in the dynamic system with constant local kinetic coefficients during successive bifurcations point to the fact that a spontaneous symmetry breaking takes place. Figure 9 shows cross sections of the conductor in the r–z

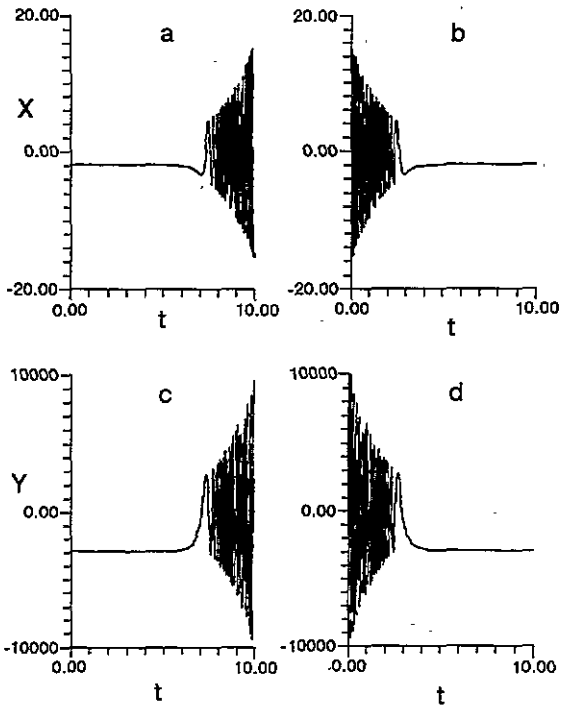

Figure 7. Time variation of the X and Y amplitudes in circuit S2 with a DC voltage source at a backward running and a forward running time: (a) $X(t)$ in the circuit with the nonlinear element at the back running time; (b) $X(t)$ in the circuit with the nonlinear element at forward running time; (c) $Y(t)$ in the circuit with the nonlinear element at backward running time; (d) $Y(t)$ in the circuit with the nonlinear element at forward running time.

plane at characteristic times marked by * on the curve $S(t)$ (see figure 5(a)). Figure 9(a) presents the initiation of a double stationary point of the dynamic system 'centre-saddle' (3) (the moment of the first vortex set initiation) and figure 9(b) shows the second vortex set initiation. From the moment of the first vortex set initiation, a separatrix surface forms, which divides the region occupied by the current into two parts, with part of the total current being partly 'intercepted' by vortices. Sites marked by * in figure 9(a), correspond to the location of a Joule heating source due to the disturbance of the conductor uniformity. These sites correspond to the so-called 'hot points' revealed in electrically explosive conductors [15] (we will discuss them in detail in the third paper of the present series). During a further evolution the region occupied by a laminar current is 're-squeezed' (figures 9(c) and (d) show the field of the separatrix at the onset and at the end of the commutation, respectively).

Thus, the increase in the effective conductor resistance is a consequence of the change in the topology of the conductor region occupied by the current and not an increase in a local specific resistance that is caused by small-scale kinetic fluctuations.

Figure 9(e) corresponds to the first connection of current in reverse polarity. One can see that it is not the change of particle rotation in the vortex which the polarity reversal corresponds to, but a reconnection of trajectories belonging to the separatrix between neighbouring couples of singular points on the external surface of the conductor. Figure 9(f) shows the field of separatrices for the state of the dynamic system close to a stationary one. It can by seen that in the stationary state a low current, sufficient to sustain the steady state in an open dissipative system, is reached. An effective turbulent conductor resistance in the stationary state is greater by two orders of magnitude than the initial one. Figure 10 shows the field of conduction electron trajectories which correspond to the time close to that in figure 9(f).

Figure 11 shows the field of hydrodynamic particle trajectories. It is easy to notice

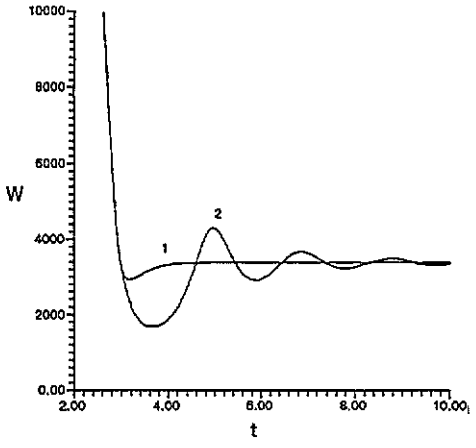

Figure 8. Time variation in the length of the radius vector of the amplitudes $W = (\sum Y_i)^{1/2}$, $\{Y_i\} = \{X, Y, Z, I\}$: curve 1, the marked trajectory (see figure 7); curve 2, the trajectory from its ε vicinity.

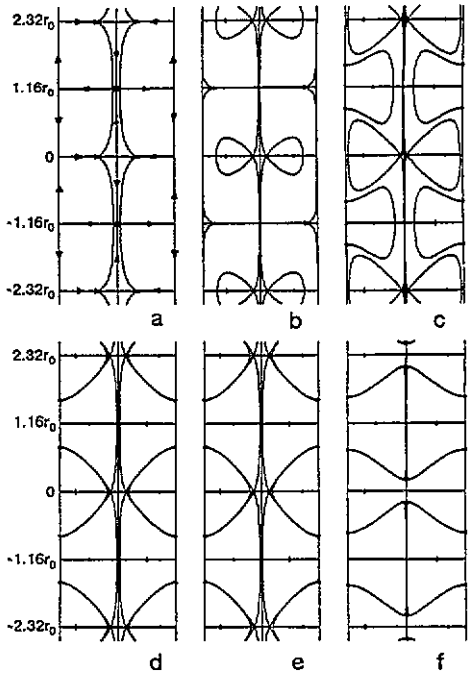

Figure 9. Cross section of the separatrix surface in the r–z plane, which separates finite trajectories of conduction electrons from infinite ones in the circuit S2 with a DC voltage source at times marked by * on the curve $S(t)$ (figure 5(a)). Sites marked by * in (a) correspond to the location of a Joule heating source; arrows in (a) direct the vector field velocity of plasma-like medium particles. The state corresponding to (f) is similar to a stationary one.

that the hot points are squeezed between hydrodynamic vortex loops, the particles of which move towards each other near the axis. It is known [16] that vortex loops can move along the loop axis, the direction of their motion coinciding with the direction of particles near the axis. Hence, vortex loops, the particles of which move towards each other near the axis, are attracted, forming pairs similar to Cooper pairs in superconductors [17], and loops, the particles of which move in opposite directions near the axis, are repelled. Due to this fact the conductor starts splitting into pieces which have (see [1]) $k_1 = 0.5k_0$ and which are topologically equivalent to the sphere without an axis. This fact allows us to understand the similarity hypothesized in [1], that, in splitting, the following hierarchy takes place: $k_2 = 2k_0 \rightarrow k_3 = 2k_2 \rightarrow k_4 = 2k_3$ etc, proceeding on the assumption that particles formed as a result of the conductor splitting 'contain' paired vortex loops.

Transition processes in circuits with a finite energy store differ essentially from those in circuits under a DC voltage, in particular, the steady state in the circuit S3 corresponds to the condition $X_\infty = Y_\infty = Z_\infty = I_{1\infty} = I_{2\infty} = 0$. Figure 12($a$) shows VCC in the circuit S3, the parameters of which are chosen so that the transition process in a subcritical regime may be close to the aperiodic one: $\Pi_0 = \Pi_1 = \Pi_3 = 1$, $\Pi_2 = 0.1$, $\Pi_4 = 0.5$, $\Pi_5 = 0.1$; $X(0) = -1.1419$, $Y(0) = Z(0) = 0$, $r_1 = 750$. The onset of a curved portion with a negative differential resistance of NE corresponds to a topological reconstruction of singular

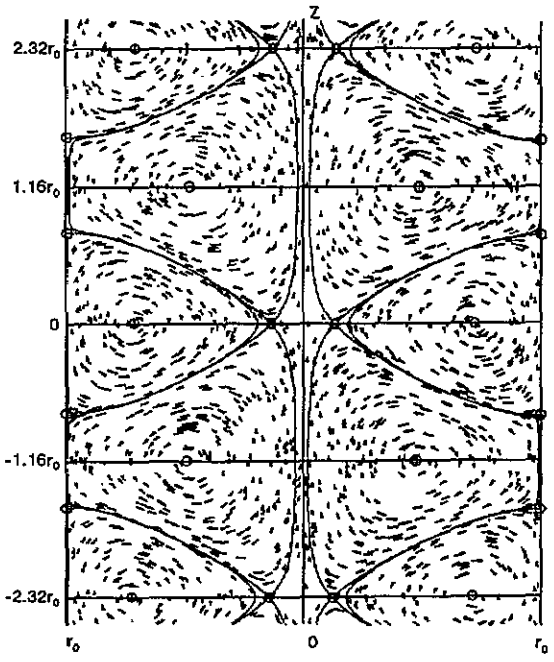

Figure 10. Vector field of the current density in the nonlinear element corresponding to figure 9(*d*): $t = 26.59$, $I = -0.906 \times 10^{-2}$, $X = -5.1398$, $Y = -2201.38$, $Z = -1797.53$. The solid curve shows the cross section of the separatrix surface in the r–z plane.

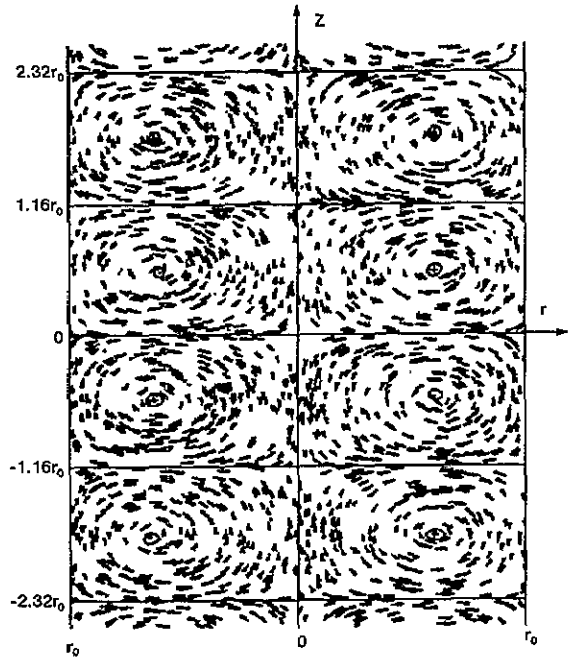

Figure 11. Vector field of the hydrodynamic velocity.

points of the dynamic system determined by (1) (see figures 12(*b*), (*c*)), in consequence of which a channel for a laminar flow along the conductor axis is formed. During the initial and decaying portions of VCC where the circuit current is low, closed toroidal structures may be formed which are ellipsoids or spheres 'dressed' on the axis which is a separatrix (figure 13).

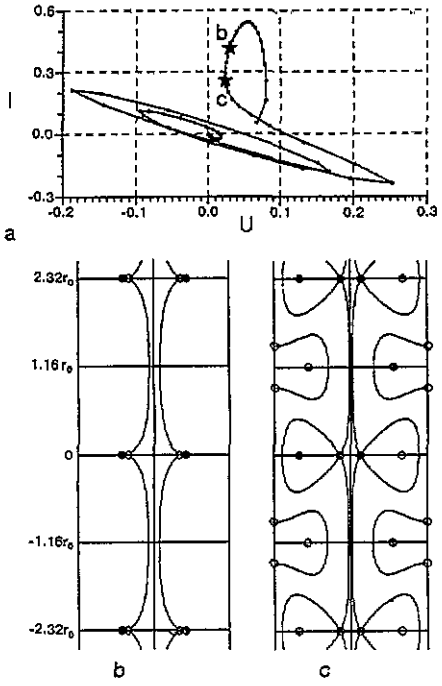

Figure 12. UI-characteristics (a), and the cross section of the separatrix surface at the moment of the first vortex system initiation (b) and at the beginning of the UI-characteristics with a negative differential resistance (c) by * in (a) in the circuit S3 with a limited energy content.

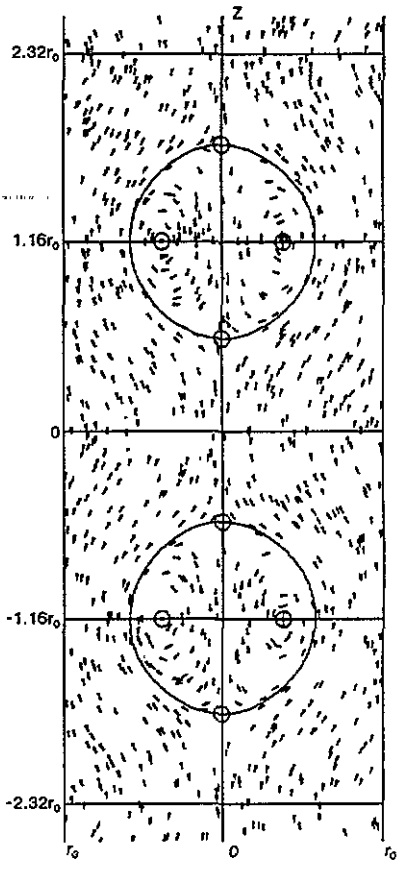

Figure 13. Vector field of the current density and the cross section of the separatrix surface during the decay section of the UI-characteristics in the circuit S3 with a limited energy content.

It should be noted that in circuits with finite energy store sources, the dynamics of the states of current and NPT are determined not only by the control parameter r_1 but also by the initial amplitude of the field of hydrodynamic velocity X which depends on the prehistory of the process (in particular, on the process of storing mechanical defects during the stage of pre-melting and melting). Since we deal with an electrodynamic system, the NFT can be realized only due to X , i.e. due to energy stored in mechanical degrees of freedom in the previous stages of the process. This idea is supported by experiments where the conductor current was interrupted while the conductor was still melting. For example, in [18] the conductor was shown to break down after about 100 μs.

For the dynamic system with backwards running time, separatrices split the current into three laminar currents; the boundaries between them are formed by separatrices with vortices, the area of which changes chaotically (in time). Figure 14(a) shows the time variation of the Kolmogorov–Sinai entropy; the point on the curve $S(t)$ corresponds to the onset of chaos. Figure 14(b) shows separatrices of conduction electron trajectories at the same time. In this case, the current and voltage drop across the conductor increase and

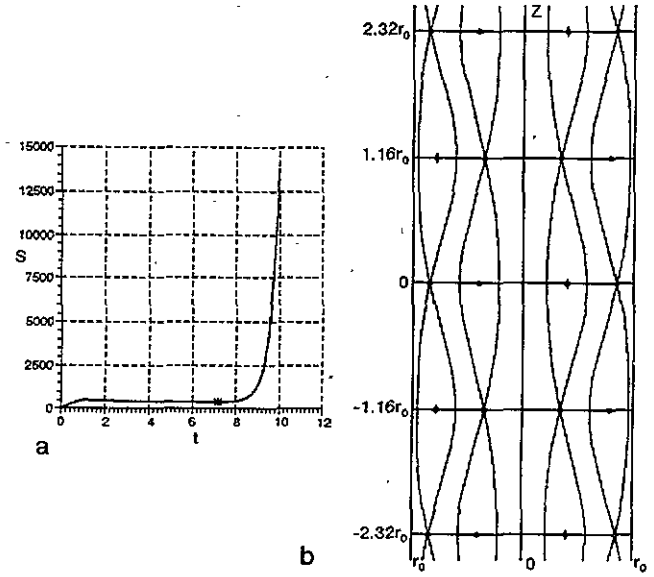

Figure 14. (*a*) Time variation of the Kolmogorov–Sinai entropy in the circuit S2 with a DC voltage source and the nonlinear element at the backward running time; and (*b*) the cross section of the separatrix surface in the r–z plane at the time marked by * on the curve $S(t)$.

the absolute impedance has a considerably smaller value than in the stationary state of the circuit S2.

Included as a component of circuits S2 and S3, a source of external noise in the form $E(t) = E\cos(\omega t + \varphi)$ with a deterministic or random phase (uniformly distributed in the space $[0, 2\pi]$) enabled investigation of NPT induced by external noise. In the circuit S2 under a DC voltage, time intervals between bifurcations were shown to increase under the action of deterministic noise. In addition, the transition process in the intervals is basically determined

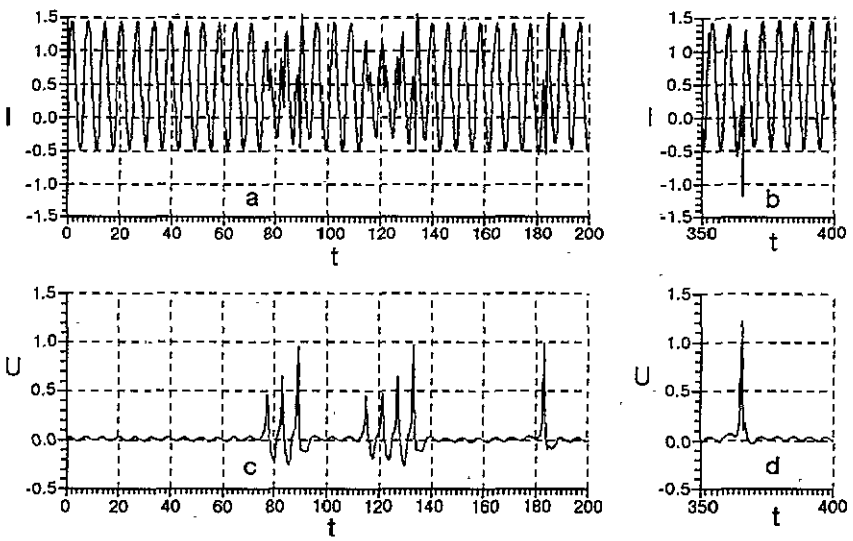

Figure 15. (*a*), (*b*) Time variation in the current of the nonlinear element; and (*c*), (*d*) the voltage across this element in circuit S2 with a DC voltage source and with an additional source of external harmonic noise.

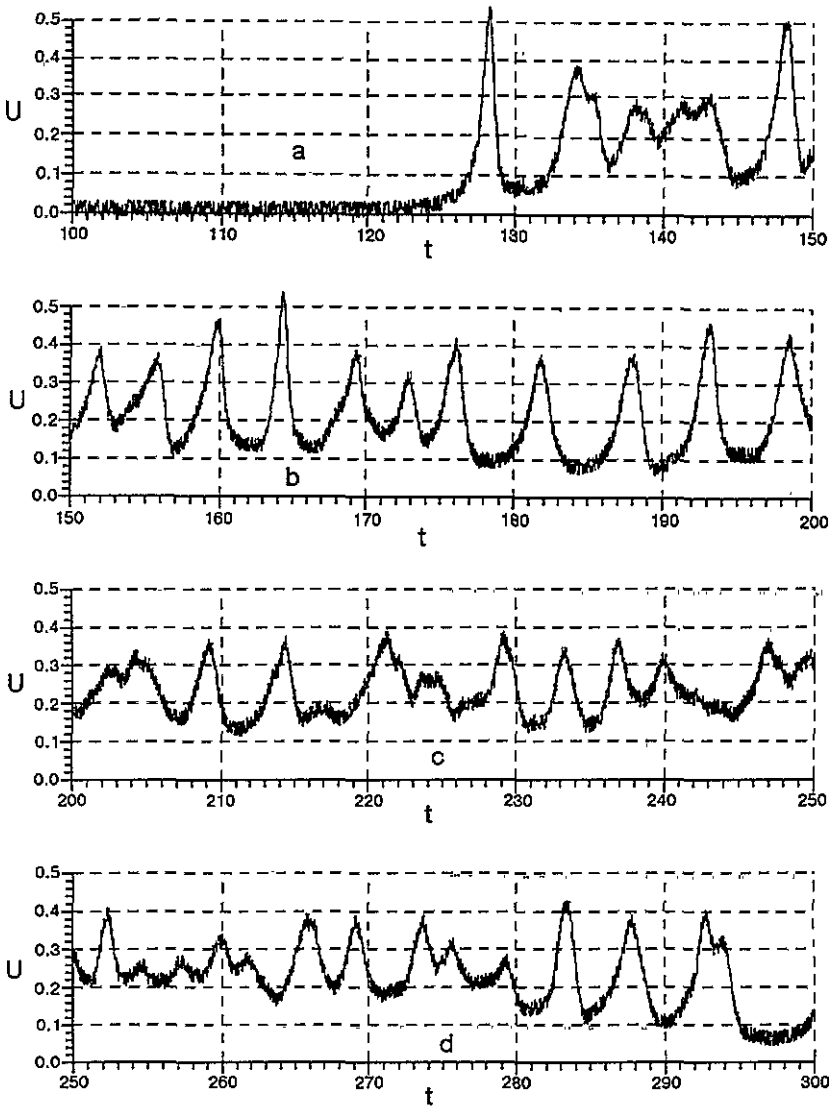

Figure 16. Time variation in the voltage across the nonlinear element in the circuit S2 with a DC voltage source and with an external harmonic voltage source having a random phase distributed in the interval $[0, 2\pi]$ with the probability $w = (2\pi)^{-1}$: (a), (b), (c) and (d) correspond to various time intervals.

by an external harmonic EMF (see figure 15, exhibiting the change in current and voltage in NE). The harmonic perturbation can be seen to destroy the stationary state in circuit S2 under a DC voltage by hindering a non-equilibrium phase transition (decreasing the degree of supercriticality) and by changing the form of the resulting current and voltage pulses. In the intervals between bifurcations the existence of topological structures characteristic of sources with a finite store of energy is possible and the effective resistance of NE is close to the initial one.

Exposed to a harmonic EMF with a random phase, stochastic oscillations are brought about in circuit S2 and their behaviour is determined not only by a random phase transition

but also by bifurcations. In addition, in the intervals between the latter, the effective resistance of NE does not reach its initial value (figure 16).

In circuit S3 under a DC voltage, the stationary state represents a limiting cycle with a known frequency (in our case $\omega = 0.4\pi$). It is interesting to study the influence of EMF having the same frequency and the detunings of frequency on processes in the dynamic system. Figures 17–19 show point mappings of the dynamic system in the I_1–I_2 plane for different time intervals. It can be seen that when affected by an EMF with a resonant frequency, the transition chaos takes a finite time at the end of which the limiting cycle is formed, representing a finite digital set of points. Hence, the fractal dimension is smaller than the dimension of phase space. The detuning of the frequency results in the appearance of chaotic fluctuations which are qualitatively similar to those appearing under the influence of a harmonic EMF with a random phase.

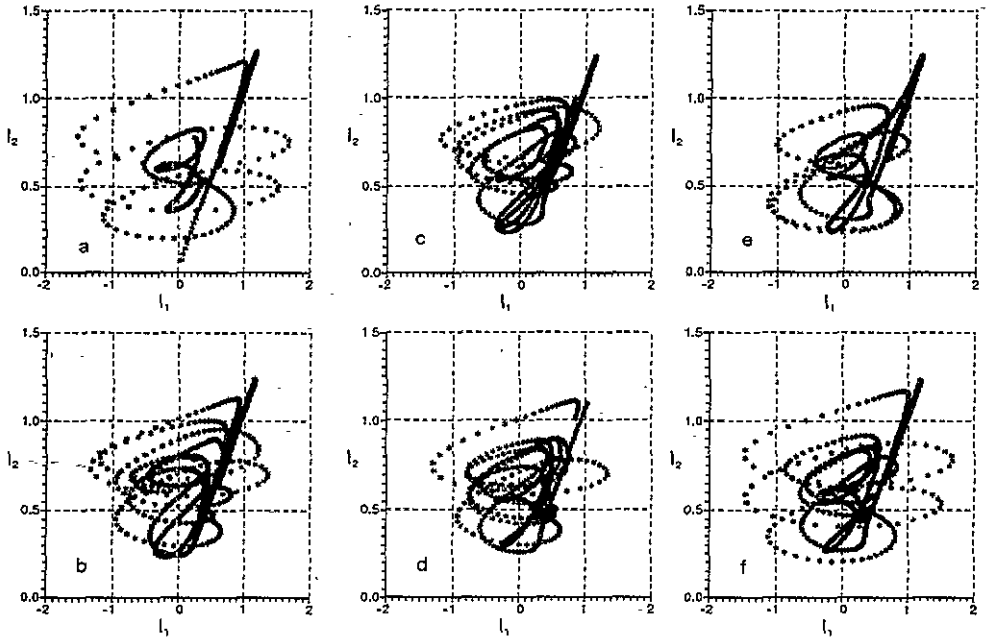

Figure 17. Point mapping of the phase trajectory in the plane I_2–I_1 in circuit S3 with a DC voltage source and an external harmonic noise voltage source with frequency $\omega = 0.2\pi$: (*a*) $t \in [0, 50]$; (*b*) $t \in [50, 100]$; (*c*) $t \in [100, 150]$; (*d*) $t \in [150, 200]$; (*e*) $t \in [200, 250]$; (*f*) $t \in [250, 300]$.

4. Conclusion

The principal result of the present paper is a demonstration that large-scale vortex perturbations determine the dynamics of states of current in plasma-like media. It is important that the conductor material is supposed to be incompressible and local kinetic coefficients are constant. Hence, we have a sufficiently simple analogy with equilibrium phase transitions, where a local potential of interaction between particles does not influence practically the dynamics of the phase transition [19]. The results obtained and discussed

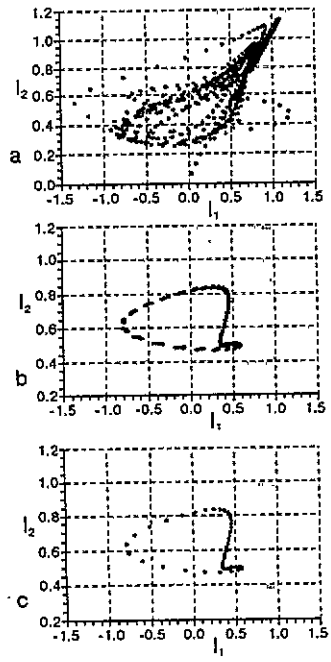

Figure 18. Point mapping of the phase trajectory in the plane I_2–I_1 in circuit S3 with a DC voltage source and an external harmonic noise voltage source with frequency equal to the natural frequency ($\omega = 0.4\pi$): (*a*) $t \in [0, 100]$; (*b*) $t \in [100, 200]$; (*c*) $t \in [200, 300]$.

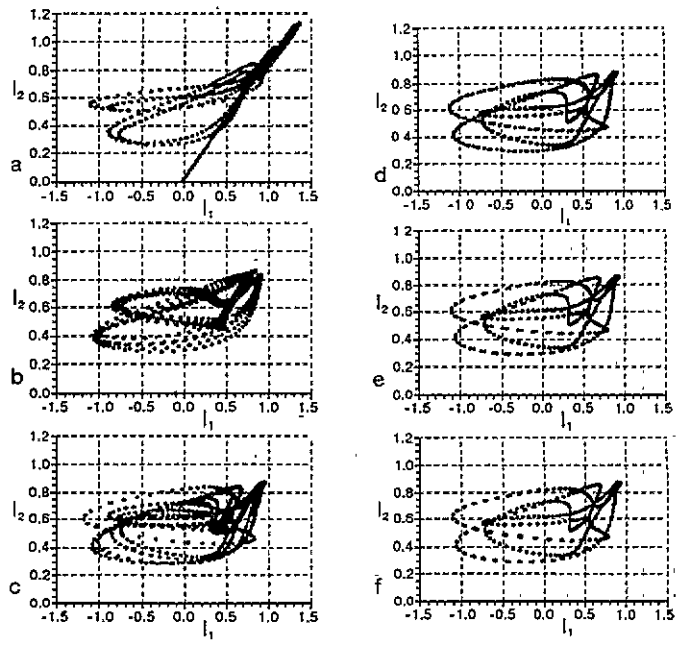

Figure 19. Point mapping of the phase trajectory in the plane I_2–I_1 in circuit S3 with a DC voltage source and an external harmonic noise voltage source with frequency $\omega = 0.6\pi$: (*a*) $t \in [0, 50]$; (*b*) $t \in [50, 100]$; (*c*) $t \in [100, 150]$; (*d*) $t \in [150, 200]$; (*e*) $t \in [200, 250]$; (*f*) $t \in [250, 300]$.

above are mostly of a qualitative character, as they are not applicable from the beginning of the space scale splitting. Nevertheless, they can be applied in a qualitative analysis of experiments on the electrical explosion of conductors discussed in the third paper of our series.

Acknowledgments

We are pleased to thank A I Tebaikin and D A Kargapolov for assistance during the computer experiment and the opportunity to use the computer graphics software developed by them.

References

[1] Volkov N B and Iskoldsky A M 1993 *J. Phys. A: Math. Gen.* **26** 6635
[2] Volkov N B and Iskoldsky A M 1990 *JETP Lett.* **51** 634
[3] Anosov D V and Arnold V I (ed) 1988 *Dynamical Systems 1. Ordinary Differential Equations and Smooth Dynamical Systems* (New York: Springer)
[4] Sinai Ya G (ed) 1989 *Dynamical Systems 2. Ergodic Theory with Applications to Dynamical Systems and Statistical Mechanics* (New York: Springer)
[5] Arnold V I, Varchenko A N and Gusein-Zade S M 1982 *Singularities of Differentiable Mappings 1. Classification of Critical Points, Caustics and Wave Fronts* (Moscow: Nauka) (in Russian)
[6] Arnold V I, Varchenko A N and Gusein-Zade S N 1984 *Singularities of Differentiable Mappings 2. Monodromy and Integral Asymptotic* (Moscow: Nauka) (in Russian)
[7] Bautin N N and Leontovich E A 1984 *Methods and Technique of a Qualitative Study of the Dynamic Systems on the Plane* (Moscow: Nauka) (in Russian)
[8] Benettin G, Galgani L and Strelcyn J M 1976 *Phys. Rev.* A **14** 2338
[9] Benettin G, Froeschle C and Scheidecker J P 1979 *Phys. Rev.* A **19** 2454
[10] Zaslavsky G M 1984 *Stochasticity on the Dynamical Systems* (Moskow: Nauka) (in Russian)
[11] Krylov N S 1979 *Works on the Foundation of Statistical Physics* (Princeton, NJ: Princeton University Press)
[12] Kaplan J L and Yorke J A 1979 *Lecture Notes in Maths* **730** 204
[13] Zaslavsky G M and Sagdeev R Z 1988 *Introduction to Nonlinear Physics* (Moscow: Nauka) (in Russian)
[14] Young L C 1969 *Lectures on the Calculus of Variations and Optimal Control Theory* (Philadelphia, PA: Sounders)
[15] Baksht R B, Datzko I M and Korostelev A Ph 1985 *JTP* **55** 1540 (in Russian)
[16] Lamb H 1932 *Hydrodynamics* (Cambridge: Cambridge University Press)
[17] Cooper L N 1956 *Phys. Rev.* **104** 1189
[18] Abramova K B, Zlatin N A and Peregood B P 1975 *JETP* **69** 2007 (in Russian)
[19] Landau L D and Lifshitz E M 1969 *Statistical Physics* (Massachusets: Addison-Wesley)